

## Skin Friction CFD Calculation for Complex Flow: Turbulent Flow along an External Corner

K. A. M. Moinuddin<sup>1</sup> P. N. Joubert<sup>2</sup> and M. S. Chong<sup>2</sup>

<sup>1</sup> Centre for Environmental Safety and Risk Engineering  
Victoria University of Technology, PO Box 14428, Melbourne City MC, VIC-8001 AUSTRALIA

<sup>2</sup>Department of Mechanical and Manufacturing Engineering  
The University of Melbourne, VIC-3010 AUSTRALIA

### Abstract

RSM (Reynolds Stress Model) simulations of turbulent flow on a streamwise external corner were carried out using the CFD code FLUENT to obtain skin friction. Both wall function and near-wall treatment approaches were used. Experimental data from an earlier experimental study [J. Fluid Mech. 511 (2004) 1], measured at the streamwise station  $x = 0.54$  m was used as the inlet condition for the numerical simulation. The objective of the numerical investigation is to determine the accuracy of RSM prediction of skin friction coefficients ( $C_f$ ) for a complex three-dimensional flow. Calculated values were compared with the experimental data and only wall function model data is found to be in reasonable agreement.

### Introduction

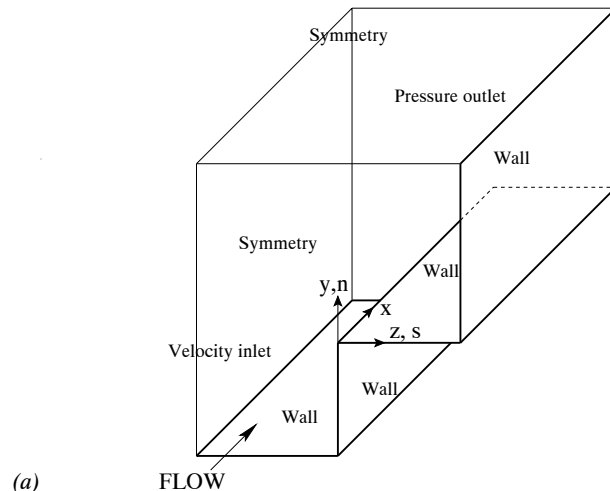
Commercial CFD softwares are widely used to calculate various forms of drag in number of engineering applications. Most of these applications are complex in nature. Since experimental investigation of complex flow, such as turbulent flow along an external corner has been conducted [1, 2], it is worthwhile to find whether CFD calculations can replicate the measured skin friction data.

In the earlier studies of [1, 2] the details of turbulent boundary layer development over a 6 m long external corner were investigated using hot-wire anemometry in a large closed circuit wind tunnel. Mean streamwise velocities were also measured using a Pitot-static tube. The first measurement point of the mean velocity profile was taken as Preston tube measurement of  $C_f$ . This quantity was also calculated using a Clauser chart. Details are presented in [1].

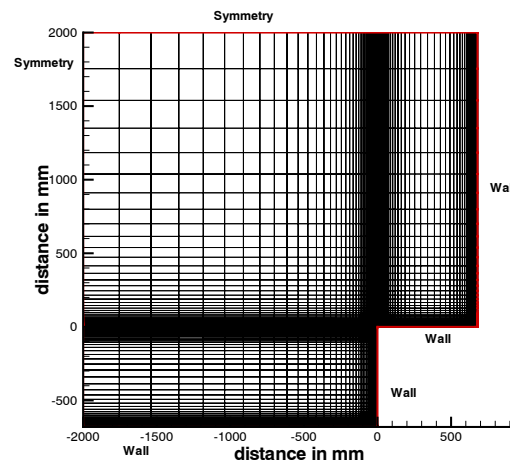
For this numerical simulation a commercial Computational Fluid Dynamics (CFD) software, FLUENT 6.0, was used adopting a Reynolds Stress Model (RSM). For the details of the numerical scheme, grid configuration and boundary conditions, refer to [3]. A brief description with emphasis to grid configuration is presented in the next section. In FLUENT calculation, wall can be treated with three different approaches: (a) near-wall model (based on [4, 5]), (b) standard wall function model [6] and (c) non-equilibrium wall function model [7]. The current study utilizes all three models.

### Numerical technique

Incompressible turbulent flow along streamwise corners was considered. The geometry and co-ordinate systems are displayed in figure 1(a). Two different sets of grids (one consisting of 588,000 and the other of 507,000 hexahedral elements) were generated. The first set was created for the near-wall RSM model, where the grids are clustered closely to the wall to ensure that the first computational node is at  $y^+ < 5$  (for the current study  $y^+ \approx 1$ ) as per FLUENT guidelines (assuming that the  $u^+ = y^+$  relationship exists in that region). In addition, a very



(a)



(b)

Figure 1: (a) Flow configuration of streamwise corner for numerical simulation (not to scale). (b) Mesh distribution on the cross section of the flow domain. Figures are presented looking upstream.

fine grid was generated near the streamwise corners to capture the correct secondary flow structures.

Traditionally, in most of the commercially available CFD codes, including FLUENT, the preferred mode of simulation is the wall function approach. For this approach, FLUENT suggests that the first computational grid should be set at  $30 < y^+ < 60$  (assuming that log-law exists in that region). This necessitates the need for the second set of grids with the first computational

node at  $y^+ \approx 30$ . The same guideline applies for both standard and non-equilibrium wall functions.

Experimental data measured at the streamwise station at 0.54 m was used as the inlet condition for the numerical simulation. Off-the-wall boundary conditions are normally used for both near-wall and standard wall function approaches in FLUENT. In the wall function approach (both standard and non-equilibrium), the viscosity-affected region is not resolved. Instead, semi-empirical formulae known as “wall functions” are used to bridge the viscosity-affected region between the wall and the fully turbulent region. To compute the values of the mean velocity components, Reynolds stresses and dissipation rate ( $\epsilon$ ) at the first node off-the-wall separate wall functions are used. In the near-wall model the viscosity-affected region is usually resolved all the way to the wall. However, similar to the standard wall functions, enhanced wall functions are used to compute the quantities at the first grid off-the-wall for the FLUENT near-wall model. This is a deviation from the original Launder and Shima model [8], where flow to be calculated all the way down to the wall, setting zero values of all the velocity and Reynolds stress components. These boundary conditions have been discussed elaborately in [3]. The convergence of the calculation is determined by monitoring the residual versus iteration curves. The simulations are conducted until these curves are flattened.

## Results

In figure 2(a), the spanwise  $C_f$  profiles, at  $x=4.565$ m, from all three runs (simulations) are plotted. In addition, near-wall method data from [3] is shown, in which  $y^+ \approx 3$ . All profiles have similar trends, except very close to the corner. Unexpectedly, near-wall method values are much higher than the wall function method values. The FLUENT near-wall model calculates wall shear stress based on the assumption that the law  $u^+ = y^+$  exists in the viscous sublayer. Therefore, despite calculating approximately correct values of the mean velocity, a very minor inaccuracy may result in an erroneous local skin friction coefficient ( $C_f$ ). Although emphasis is given on the importance of setting  $y^+ \approx 1$  in [5], a simulation with  $y^+ < 5$  does not provide much variation.

In figure 2(b) all the current numerical profiles, as well as profile from [9], are normalised by  $C_{f2D}$ , the  $C_f$  value in the 2-D region. A length scale  $s_{2D}$  is also used, which represents spanwise distance from the corner where the nominal 2-D region approximately starts. For the [9] profile  $s_{2D}$  is the distance between the corner and the wall bisector. The profiles are found to have excellent similarity, except very close to the corner. Besides differences in flow geometry, the study of [9] adopted a coarse grid for the external corner. All these may have contributed to the larger difference close to the corner.

The  $C_f$  is usually measured in mild 3-D flows using a Preston tube. The experimental data of [1] (obtained using a Preston tube) is compared with both wall function model data in figure 3. Overall a very good agreement is observed. However, data from the near-wall model is not plotted in this figure. Correlating figure 2(a), it is clear that the near-wall model grossly overpredicts  $C_f$  values all along the model.

Unlike the experimental finding, at  $x=1.07$  m multiple peaks are not found in the numerical profiles and the values of the peaks (close the corner) are smaller compared to the experimental data. Overall the non-equilibrium model better predicts the data at this station compared to standard wall function model.

In figure 4, the comparison of both wall function model data with the experimental data (obtained using a Clauser chart) is

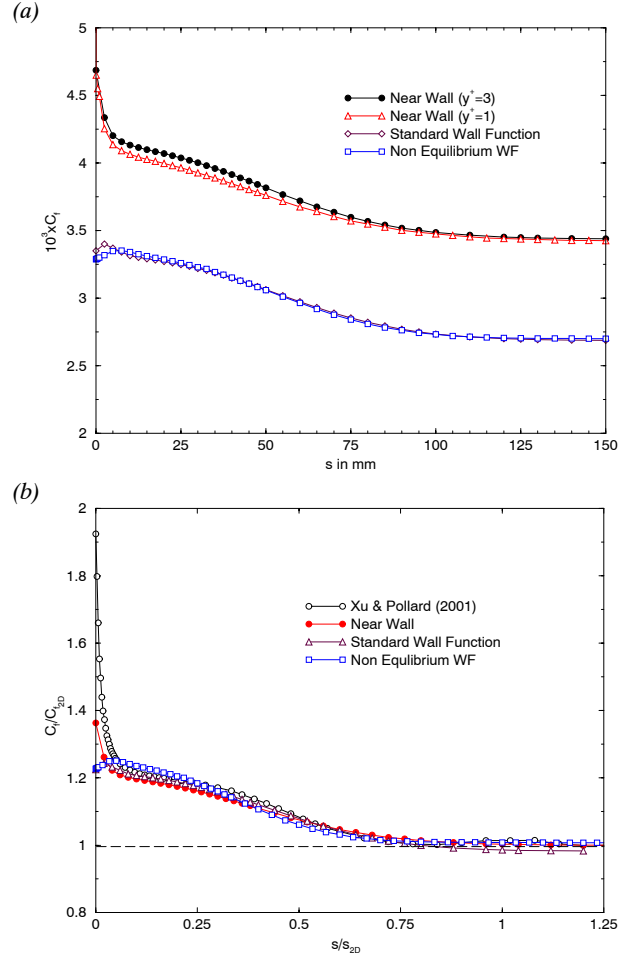


Figure 2: (a) Comparison between absolute spanwise  $C_f$  profiles from all current numerical simulations. (b) Comparison of normalised spanwise  $C_f$  profiles from current numerical simulations and [9].  $s_{2D}$  represents spanwise distance from the corner where the nominal 2-D region approximately starts.

presented for five streamwise stations. The numerical data is found to be significantly lower compared to the experimental data derived from a Clauser chart. This difference is larger at the upstream stations (i.e.  $x=1.07$  m and 2.17 m) compared to the downstream stations. However, at  $x=1.07$  m prediction by non equilibrium model is comparatively better. The difference between the wall function data and the Clauser chart data is the same order of magnitude as the difference between the Clauser chart data and the Preston tube data, which is given in the fourth column of table 1.

2-D values for $C_f$ distribution			
Station (in mm)	Clauser Chart	Preston tube	Diff.
$x, s=1070, 40$	$3.637 \times 10^{-3}$	$3.315 \times 10^{-3}$	9.71
$x, s=2170, 100$	$3.087 \times 10^{-3}$	$2.869 \times 10^{-3}$	7.07
$x, s=3385, 100$	$2.941 \times 10^{-3}$	$2.765 \times 10^{-3}$	6.70
$x, s=4565, 100$	$2.880 \times 10^{-3}$	$2.735 \times 10^{-3}$	5.30
$x, s=5010, 100$	$2.878 \times 10^{-3}$	$2.731 \times 10^{-3}$	5.38

Table 1:  $C_f$  values in the nominal 2-D region at various streamwise station. distribution. The fourth column shows the difference between two methods as a percentage.

Although in the experimental study, the shape of the spanwise  $C_f$  profile are different at early and downstream streamwise

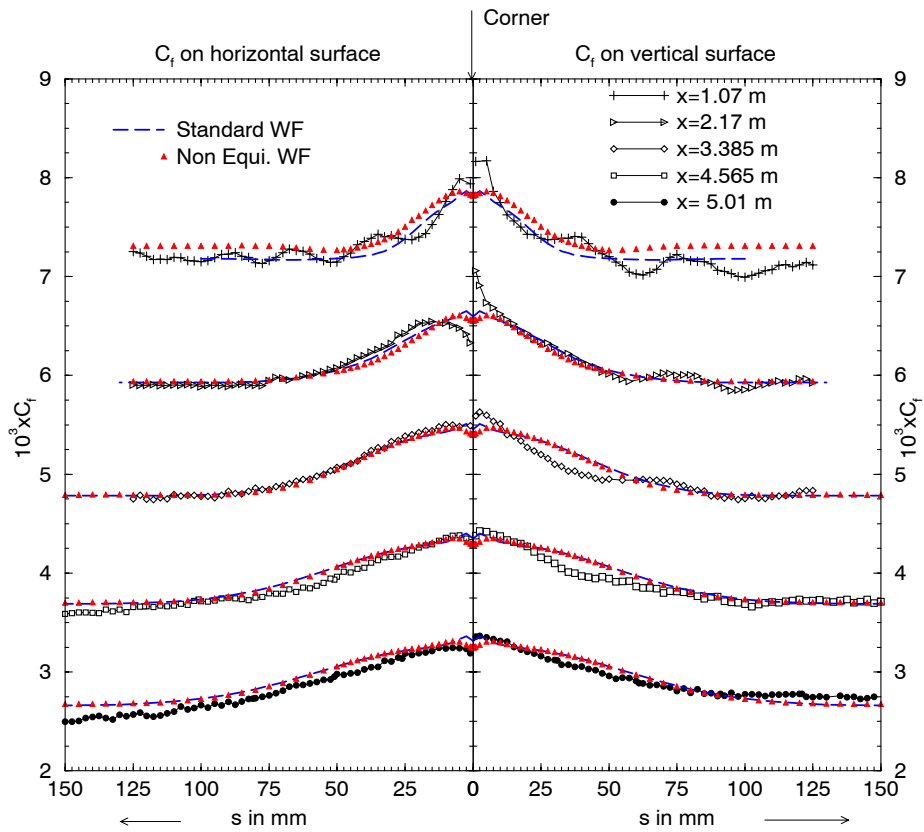


Figure 3: Comparison of spanwise  $C_f$  profiles from both wall function model simulations with that from the experimental data (based on Preston tube). Profiles for each streamwise station are shifted 1 unit upwards from the downstream one except at  $x=5.01$ m.

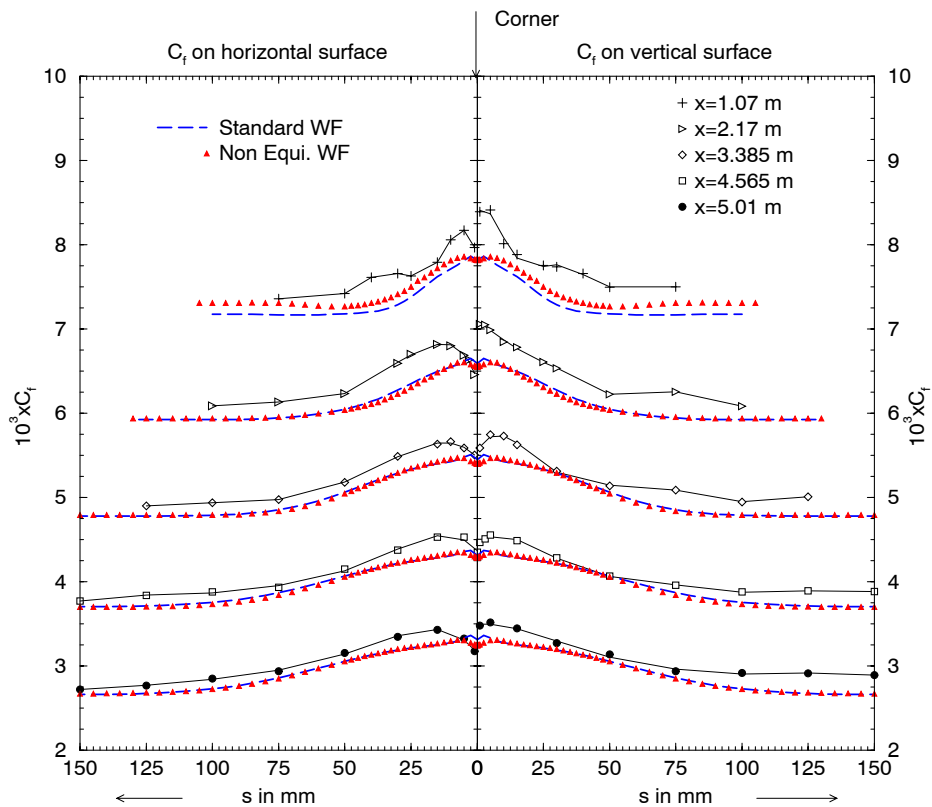


Figure 4: Comparison of spanwise  $C_f$  profiles from both wall function model simulations with that of experimental data (derived from a Clauser chart). Profiles for each streamwise station are shifted 1 unit upwards from downstream one except at  $x=5.01$ m.

stations (presented in [1]), these profiles are found to have a similar shape all along the model in the numerical study. It is observed that similar to the experimental findings, in the numerical studies with wall function model, the maximum value of  $C_f$  occur away from the streamwise corner. As one moves away from the location of the maximum, the  $C_f$  decays exponentially towards the two-dimensional region. The location of the maximum  $C_f$  from the standard wall function model data is found to be closer to the corner ( $s \approx 2.5$  mm) compared to that from the experimental findings ( $s < 5$  mm at early station and  $s < 10$  mm downstream). However these locations from the non-equilibrium model are found to be similar to that from the experimental study.

### Conclusions

Numerical simulation based on an RSM model is performed for the flow along an external corner. The current study shows that in an ideal situation the boundary layer develops symmetrically about the external corner bisector and therefore, the  $C_f$  distribution is symmetrical too. The  $C_f$  distribution from the wall function model simulation is found to be in reasonable agreement with the experimental work. However, the near-wall model simulation grossly overpredicts the  $C_f$  values. This problem has been traced back by [3] to the fact that a serious error is involved with the wall boundary conditions (enhanced wall functions) for Reynolds stresses. Therefore, it is suggested that for the near-wall model, instead of using off-the-wall boundary conditions, flow to be calculated all the way down to the wall setting zero values of all the velocity and Reynolds stress components (as done in [8]).

### Acknowledgements

The authors gratefully acknowledge the assistance of Dr. A. Ooi for his valuable advice during this study.

### References

- [1] Moinuddin, K. A. M., Joubert, P. N., Chong, M. S. and Hafez, S. Experimental investigation of turbulent boundary layer developing along a streamwise external corner (Chine), *Exp. Thermal and Fluid Science*, **27(5)**, 2003, 599–609.
- [2] Moinuddin, K. A. M., Joubert, P. N. and Chong, M. S. Experimental investigation of turbulence-driven secondary motion on a streamwise external corner. *J. Fluid Mech.*, **511**, 2004, 1–23.
- [3] Moinuddin, K. A. M., Joubert, P. N., A. Ooi and Chong, M. S. RSM Simulation of turbulence-driven secondary motion over a streamwise external corner: Comparison with experimental result *Trans. ASME I, J. Fluid Eng.* (under review).
- [4] Chen, H. C. and Patel, V. C. Near-wall turbulence models for complex flows including separation. *AIAA Journal* **26(6)**, 1988, 641–648.
- [5] Malan, P. and Kim, S.-E. A unified wall treatment for turbulent flows-Part 1: Hydrodynamics. *Fluent Internal Publication* January, 2000 (unpublished).
- [6] Launder, B. E. and Spalding, D. B. The numerical computation of turbulent flows. *Comput. Methods Appl. Mech. Eng.* **3**, 1974, 269–289.
- [7] Kim, S.-E. and Choudhury, D. A near wall treatment using wall functions sensitized to pressure gradient. In *ASME FED Vol. 217, Separated and Complex Flows*. ASME, 1995.
- [8] Launder, B. E. and Shima, N. Second-moment closure for the near-wall sublayer: Development and application. *AIAA Journal* **27(10)**, 1989, 1319–1325.
- [9] Xu, H. and Pollard, A. Large eddy simulation of turbulent flow in a square annular duct. *Phys. Fluids*, **13**, 2001, 3321–3337.